INTERNATIONAL JOURNAL OF EARTH AND ATMOSPHERIC SCIENCE
Journal homepage: www.jakraya.com/journal/ijeas

ORIGINAL ARTICLE

Identification of Aerosol Sources and Its Characterization at Varanasi: An Air Mass Based Study

S. Tiwari[1*, 2], R.K. Singh[3], A.K. Srivastava[4], V.K. Soni[5], Suresh Tiwari[4], R.S. Singh[6], M.K. Srivastava[3] and A.K. Singh[1, 7]

[1]Atmospheric Research Laboratory, Department of Physics, [3]Department of Geophysics, [6]Department of Chemical Engineering, Indian Institute of Technology, [7]DST - Mahamana Centre of Excellence in Climate Change Research, Banaras Hindu University, Varanasi, India.
[2]Graduate School of Environmental Studies, Nagoya University, Japan.
[4]Indian Institute of Tropical Meteorology (Branch), Prof Ramnath Vij Marg, New Delhi, India.
[5]India Meteorological Department, Lodhi Road, New Delhi, India.

[*]Corresponding Author:

S. Tiwari

Email: pshanitiwari@gmail.com

Submitted: 04/01/2018
Accepted: 22/03/2018

Abstract

A continuous aerosol measurement were carried out at Varanasi, during 2011 using ground based hand-held sunphotometer. A discrimination of aerosol characteristics was made over the station based on their possible sources, identified from air mass back trajectory analyses at 1000m altitude above mean sea level. Four different types of source sectors were identified, viz. Type I (mainly from north-east India), Type II (mainly from north-west India like Haryana and Punjab), Type III (mainly from Middle East and Thar Desert region due to the long range transportation mixed with anthropogenic aerosol), and Type IV (mainly from the central and south India and also from oceanic region (from the Bay of Bengal), with annual contributions of nearly 9%, 32%, 36%, and 23%, respectively to the total aerosol loading. These aerosol types show a strong seasonal heterogeneity in contributions depending on their emission sources. Type II aerosols are dominated in post-monsoon (~61%) and winter (~46%) seasons while Type III aerosols are dominated in pre-monsoon (~40%) and winter (~48%) seasons. We found that local/anthropogenic aerosols are more dominant than long range transported aerosols and play crucial role in suitable meteorological condition. The measured aerosol optical properties such as aerosol optical depth (AOD) and Ångström exponent (AE) were analyzed for the identified sectors of aerosol sources to understand their detailed characteristics over the station. The annual mean value of AOD (AE) for Type I, Type II, Type III, Type IV aerosols are 0.98±0.31 (0.93±0.26), 0.89±0.30 (1.06±0.22), 0.76±0.30 (0.92±0.25), 0.76±0.32 (0.88±0.30), respectively. The curvature study has been also carried out to corroborate the observed results**.** The direct aerosol radiative forcing was found to be maximum at the atmosphere (ATM) and top of the atmosphere (TOA) for Type III aerosol with maximum heating rate 2.89±0.30 K day^{-1}.

Keywords: Aerosol types, Air mass, Ångström exponent, Heterogeneity, Indo-Gangetic Basin.

1. Introduction

Atmospheric aerosols along with trace gases are the major constituents of atmosphere, which play vital role in Earth's climate system (Jacovides *et al.*, 1996; Kaufman *et al*., 2002; Morgan *et al*., 2006; Kaskaoutis *et al.*, 2007a; IPCC, 2007, 2013; Seinfeld *et al*., 2016). In last few decades, aerosols are recognized as a major source in determining climate change (Wild, 2009) as they influence the Earth's climate system directly by scattering and absorbing the solar and terrestrial radiations (Satheesh *et al.*, 2006; Gautam *et al.*, 2010; Srivastava *et al*., 2014) and indirectly by forming the clouds and modifying their macro and micro-physical properties (Twomey, 1991; Altaratz *et al.*, 2014;

Sarangi *et al.,* 2017). Aerosols properties (both physical and chemical) show a large spatial as well as temporal variation due to different emission sources, chemical composition and their transported pathways resulting some significant impacts on air quality and earth climate system (Tiwari *et al.,* 2015; Sarangi *et al.,* 2017; Sharma *et al.,* 2017; Zhao *et al.,* 2017). The climatic effects of aerosols are closely related to their optical properties, surface albedo and the relative position in respect to that of clouds (Koch and Del Genio, 2010; Kaskaoutis *et al.,* 2011; Srivastava *et al.,* 2014; Kant *et al.,* 2017). The uncertainty in determination of radiative forcing due to aerosol is no doubt decreases at global level but it is still quite uncertain at regional level. The uncertainty in aerosol radiative forcing at regional level scale is mainly because of their significant heterogeneity in spatial and temporal distribution and inadequate information about the optical and radiative characteristics of their types/compositions (IPCC, 2007, 2013). Heterogeneity in aerosol distribution may lead to different aerosol types at both regional as well as global level with significant climate response from negative (cooling) to positive (heating) (Kaskaoutis *et al.,* 2007b; Srivastava *et al.,* 2011, 2014; Tiwari *et al.,* 2016, 2015, 2013). Thus, the characterization of aerosol in the aspect of different aerosol types may reduce the uncertainty in earth's climate system and will be helpful in the improvement of climate modelling.

The Indo-Gangetic Basin (IGB) region traversed by the Ganga river and its tributaries is one of the largest, densely populated, industrialized and developing region of the world where aerosol not only affect the Indian monsoon but also the global climate system (Satheesh *et al.,* 2006). The region is of great research interest due to its unique topography surrounded by the Himalayas to the north, moderate hills to the south, Thar Desert and Arabian Sea in the west, and Bay of Bengal in the east (Prasad *et al.,* 2006; Tiwari *et al.,* 2013). The topography of IGB and variable meteorological condition control the dynamic behaviour of atmospheric aerosol in space as well in time. IGB is dominated by the urban/industrial aerosols (Guttikunda *et al.,* 2003; Sharma *et al.,* 2014; Monkkonen *et al.,* 2004; Tiwari *et al.,* 2009), which demonstrate significant seasonal variability based on the complex combination of anthropogenic factors mixed with the contribution from the natural sources (mostly dust), particularly during the pre-monsoon period (Srivastava *et al.,* 2012a; Tiwari *et al.,* 2013). With the increase in population density and energy demands, aerosol emissions have been gradually increasing, mainly through fossil-fuel and bio-fuel combustions (Lawrence and Lelieveld, 2010). The large increase in anthropogenic aerosols over IGB is hypothesized to cause considerable changes to regional monsoonal climate (Ramanathan *et al.,* 2005; Lau *et al.,* 2006; Dey and Tripathi, 2008; Gautam *et al.,* 2010; Das *et al.,* 2015). Numerous studies using satellite observations and ground-based measurements have revealed an overall increase in aerosol optical depth (AOD) over India, especially in IGB (Sarkar *et al.,* 2005; Porch *et al.,* 2007; Lawrence and Lelieveld, 2010; Dey and Di Girolamo, 2011; Kaskaoutis *et al.,* 2011; Kharol *et al.,* 2012; Ramachandran *et al.,* 2012; Mishra *et al.,* 2012; Satheesh *et al.,* 2017). Earlier studies over IGB suggest the existence of different aerosol types from various natural and anthropogenic emission sources (Sharma *et al.,* 2014; Tiwari *et al.,* 2015, 2016; Bibi *et al.,* 2017), resulting to different types of aerosol loading which have different radiative effects. Thus, for the better understanding of aerosol impacts of earth energy budget, the improvement in aerosol characterization with high spatial - temporal resolutions; particularly on the basis of aerosol type is highly needed.

The present study focuses on understanding of the aerosol characteristics over Varanasi, a semi-urban station over the eastern IGB region, for the year 2011. An attempt has been made to identify major sectors of aerosol sources over the station based on the air mass back-trajectory analysis using Hybrid Single Particle Lagrangian Integrated Trajectories (HYSPLIT) model. Furthermore, aerosol characteristic from these emission sectors and their climate impacts is also studied. Results observed in present study were found to be quite considerable with aerosol optical characteristics measured by several scientific groups throughout the world and will be useful for the climate modeler.

2. Site Description and Meteorological Conditions

Varanasi (25.20^0N, 82.90^0E and 83m above msl) is situated on the bank of river Ganga. It is a semi-urban city located at the eastern part of IGB in north India. It is heavily polluted and has high population density causing a high aerosol loading throughout the year which shows large seasonal and temporal variability (Tiwari *et al.,* 2015; Tiwari and Singh, 2013). A large scale uncontrolled urbanizations and industrial developments are the major causes for air, water and land pollution (Prasad *et al.,* 2006). Higher aerosol loading is observed over the entire IGB, including Varanasi during pre-monsoon (Singh *et al.,* 2004; Prasad *et al.,* 2007; Tiwari and Singh, 2013; Tiwari *et al.,* 2013, 2015) producing a large surface influx resulting a higher top of the atmosphere forcing and creates enough difference between surface and atmospheric forcing (Sarkar *et al.,* 2005). Recently, Tiwari and Singh (2013) reported that Varanasi

experienced different types of aerosol loading during different seasons i.e. during pre-monsoon season, coarse mode aerosol particles (mainly mineral dust) are one of the major contributors to total aerosol loading while fine-mode anthropogenic aerosols are the major contributors during post-monsoon and winter. The station is also influenced, seasonally (mainly late pre-monsoon and monsoon season) by marine aerosols. The monthly mean variation in meteorological parameters (temperature, relative humidity, wind speed and wind direction), obtain from India Meteorological Parameters (IMD), is shown in Fig 1. Figure revel a significant seasonal variability in all parameters. The minimum relative humidity is observed in April (37 ± 8 %) which continuous increases and reach maximum in August (85 ± 8 %). However, maximum temperature is observed in May (33 ± 2^0C) and decreases continuously up to minimum value January (14 ± 4^0C). During late pre-monsoon (June) and monsoon season maximum wind speed is observed which are mainly coming from the south-eastern direction. Varanasi experienced north-westerly and westerly winds from northwest India, Pakistan, and Middle East region carrying mineral dust in pre-monsoon season (Tiwari and Singh, 2013).

3. Instrumentation and Data Analysis

The ground based measurements were carried out using hand held and portable multiband sunphotometer MICROTOPS-II (Solar Light Company, USA). It contains five different interference filters at 380, 440, 500, 640, and 870 nm wavelengths and provides columnar information of aerosols. An additional channel (940 nm) is used for precipitable water vapour contents. The sunphotometer works on the principle of extension of solar radiation intensity at a certain wavelength and calculates the corresponding optical depth by using the knowledge of the solar intensity at the top of the atmosphere. The same is calculated easily by Langley method (Schmid and Wehril, 1995). The details of MICROTOPS–II, its calibration, performance and data collection method are given elsewhere (Morys *et al.,* 2001; Tiwari and Singh, 2013; Sharma *et al.,* 2014). The factory calibrated instrument was deployed and operational at the Department of Physics, Banaras Hindu University, Varanasi since January, 2011. However, in the present study, the data were analysed and studied for the year 2011. We have taken the data from morning 9:00 am to 4:30 pm at every half/or one hour on every clear sky day. During each measurement, three continuous scans are taken and processed by second order polynomial fitting and select only those data which have maximum correlation (with threshold value r>0.97) and minimum error in second order coefficient. Out of 365 days, only 239 days average AOD values have this threshold condition with 1127 numbers of data set.

4. Methodology and Theoretical Approach

Due to strong dependency of both AOD and Ångström exponent (AE) on wavelength, a realistic characterization of aerosol properties can be attempted using these two parameters (Holben *et al.,* 2001; Pinker *et al.,* 2001) and therefore, are widely used to identify different aerosol types over the globe (Tiwari *et al.,* 2015; Kaskaoutis *et al.,* 2007b). AOD and AE are the two main parameters for aerosol optical properties and the spectral variation of AOD is determined by Ångström Power law (Ångström, 1964), given by

$$\tau_\lambda = \beta\lambda^{-\alpha} \quad \ldots (1)$$

Where,

$\tau_{\lambda,}$ is AOD at wavelength λ, α is Ångström exponent and β is turbidity coefficient, which is equal to AOD at λ = 1μm. Ångström exponent is a relatively good indicator of aerosol particle size. Higher values of AE (nearly 1-3) represent the fine mode aerosol particles while lower positive as well as negative values indicate dominance of coarse mode aerosol particles (Eck *et al.,* 1999; Kaskaoutis *et al.,* 2009). The above equation (1) is a special case of more complicated equation for limited interval wavelength and particles diameter (Kaskaoutis *et al.,* 2009). Over a wide range of wavelength, Ångström formula leads to significant inaccuracies particularly when the size distribution is multimodal in vertical atmospheric column which represent the different types of aerosols coming from different sources like as biomass burning, industrial, urban, transported dust and sea salt etc. Taking the logarithms at both side of equation (1) we get

$$\ln \tau_\lambda = -\alpha \ln \lambda + \ln \beta \quad \ldots (2)$$

For two different wavelengths (λ_1 and λ_2) AE is given by

$$\alpha = -\ln (\tau_{\lambda 1} / \tau_{\lambda 2}) / \ln (\lambda_2 / \lambda_1) \quad \ldots (3)$$

The above equation implied that α is invariant in the spectral range λ_1 to λ_2. This is valid only when the size distribution of aerosols in the vertical column follows at least inverse power law (Beegum *et al.,* 2009). But, real size distributions show a variation from the power law distribution mainly when aerosol are injected from different emission sources and the spectrum has a wide range (Kaskaoutis *et al.,* 2009; Beegum *et al.,* 2009; Schuster *et al.,* 2006). Under such condition, a second order polynomial fit can be applied to AOD spectra (King and Byrne, 1976; Eck *et al.,* 1999; Kaskaoutis and Kambezidis, 2006) which can be used to quantify the curvature in spectral distribution of AODs as:

$$\ln \tau_\lambda = A_2 [\ln (\lambda)]^2 + A_1 \ln (\lambda) + A_0 \quad \ldots (4)$$

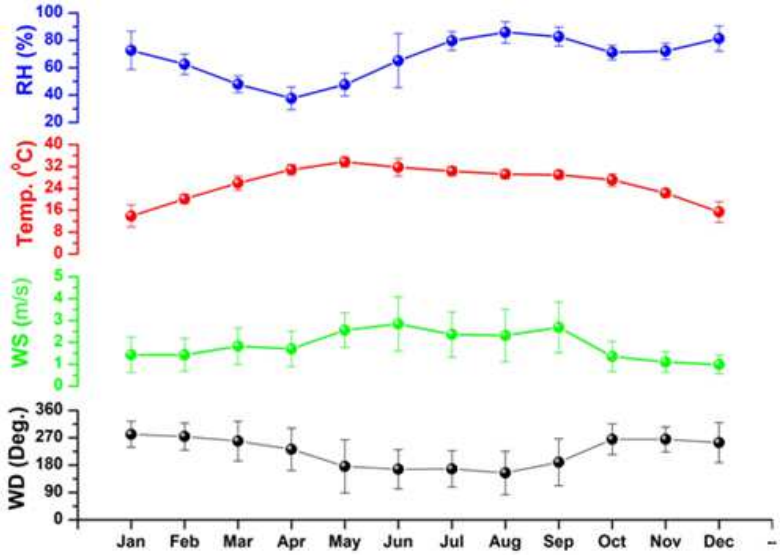

Fig 1: Monthly mean variation in meteorological parameters, i.e. (a) relative humidity, (b) temperature, (c) wind direction, and (d) wind speed, over Varanasi period during the study.

where,

Coefficient A_2 represents the curvature which is observed in measurements. It is also a very good indicator of aerosol particle size, having negative value indicates aerosol size distributions dominated by fine mode and positive value indicates size distribution dominated by coarse mode aerosol particles (Eck *et al.*, 1999; Kaskaoutis *et al.*, 2009). Although, equation (4) is more precise than equation (2) for a wide spectral range yet a large error can occurs especially in low turbidity conditions (Kaskaoutis *et al.*, 2007b). Therefore, to minimise these errors, only those data have been considered which have second order polynomial fit with r value ≥ 0.97 associated with minimum errors in curvature (A_2). In the present study, α is calculated for the pair of wavelength 380-870 nm using equation (3). To understand the optical characteristics of aerosols over Varanasi during the study period, monthly mean values of AOD (500 nm) and AE (380-870 nm) are shown in Fig 2. Nearly similar value of monthly mean AOD is found from January to July (except for March)**.** However, an increase is observed from September onwards, with a peak observed during November month, which could be due to crop residue burning (Kaskaoutis *et al.*, 2014) and/or Diwali effect (Singh *et al.*, 2014) suggesting the enhancement in fine mode aerosol particles. Further, AE is found to have two peaks, one during winter period (December, January and February) and second during post-monsoon period (October and November), which indicates the dominance of fine mode particles mainly from biomass/biofuel burning. On the other hand, during summer and monsoon period, AE values are found to be relatively lower (< 0.9), which suggests presence of coarse mode particles over the station. Tiwari and Singh (2013) also reported an enhancement in coarse and fine mode aerosol loading during pre-monsoon and post monsoon season over Varanasi.

As atmospheric aerosols show large heterogeneity over the entire IGB region and have strong spatial as well as temporal variations (Tiwari *et al.*, 2013), the region has identified with different aerosol types (Srivastava *et al.*, 2012b, 2014; Tiwari *et al.*, 2015). In several previous studies, aerosol types were identified using measured aerosol optical parameters (Kaskaoutis *et al.*, 2009; Srivastava *et al.*, 2012b, 2014; Tiwari *et al.*, 2015). However, in the present study, we identified different aerosol emission sectors associated with their different emission sources over Varanasi using air mass back-trajectory analysis at 1000 m msl altitude and investigate aerosol characteristics in each sector. The air mass back trajectories provide significant information about the emission sources of air pollutants and their transport pathways to the measurement sites. Aerosols loading and their composition at any locations are highly influenced by the meteorological parameters over particular region which affect the air mass transport. The daily 5-day air mass back-trajectories from NOAA-HYSPLIT (National Oceanic and Atmospheric Administration Hybrid Single-Particle Lagrangian Integrated Trajectory) model were analyzed (Draxler and Rolph, 2003) at Varanasi during 2011. Based on their transport pathways, four different sectors of air mass sources were identified as: Type I- mainly coming from north-east India, Type II- mainly coming

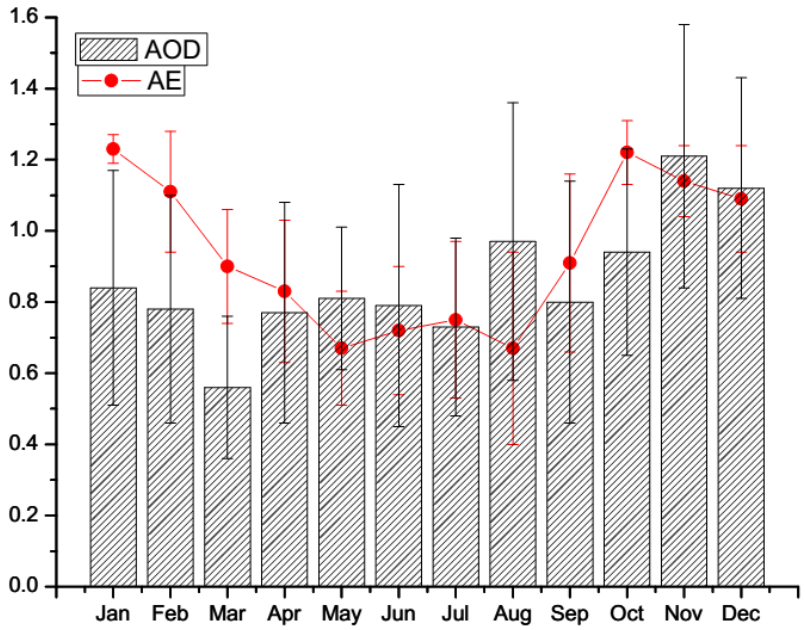

Fig 2: Monthly mean values of AOD and AE over Varanasi during 2011. The vertical lines represent the standered deviation.

from north-west India like Haryana and Punjab, Type III- mainly coming from the Middle East and Thar Desert regions due to the long-range transportation which are well admixed with anthropogenic aerosol, Type IV- mainly coming from the central and south India and also from oceanic region (mainly Bay of Bengal). The annual percentage contribution of each air mass type along with their pathways has been plotted in Fig 3. Vertical lines in each type show standard deviation, representing latitudinal spreading of air mass. Fig 3 reflects that Type I have minimum annual contribution (9.31%) while Type III have maximum annual contribution (36.16%). Apart from this, Type II and Type IV have annual contributions of 32.07% and 22.46% respectively. It was noticed from the figure that nearly 68% air masses reached at Varanasi, were mainly coming from Northern India, Middle East and Thar Desert regions. We classified the measured aerosol parameters based on inferred air masses, which are discussed in detailed in the next section.

5. Results and Discussion

5.1 Aerosol Optical Depth and Ångström Exponent for Different Aerosol Types

The characterization of aerosol particles and spectral dependence of their optical properties are important as they strongly influence the associated radiative properties (El-Metwally *et al.*, 2008; Moorthy *et al.*, 2009; Kaskaoutis *et al.*, 2011). Fig 4 represents the mean spectral variation of AOD over Varanasi for the inferred air mass types during the study period. The spectral behaviour of AOD indicates information about dominant aerosol particles (fine and coarse mode) and their size distributions etc. It was noticed from the Fig **3** that the AOD has significant spectral dependence for all types, with relatively large dependence for Type I and Type II. Similar results are observed previously by Tiwari and Singh (2013) over Varanasi and by Srivastava *et al.* (2014) over New Delhi. Figure 4 clearly reflects that Type I aerosols have maximum AOD value for all wavelengths with relatively higher steepness in slope suggesting the dominance of fine mode aerosol particles while on the other hand Type III and Type IV have nearly similar AOD values. Type III has higher value at lower wavelength associated with less spectral dependency at higher wavelength suggesting the enhancement of fine mode aerosol particles. The air masses coming from Middle East and Thar Desert due to long range transportation carrying abundance of aerosol particles which contain both fine as well as coarse mode aerosol. Due to the gravitational settling process, however, coarse particles are settled down on the pathways resulting enhancement of fine particles reached at our study site. Srivastava *et al.* (2011) also reported the enhancement of fine – mode aerosol particles over Gandhi College, Ballia during pre-monsoon season, which is nearly 140 km east from

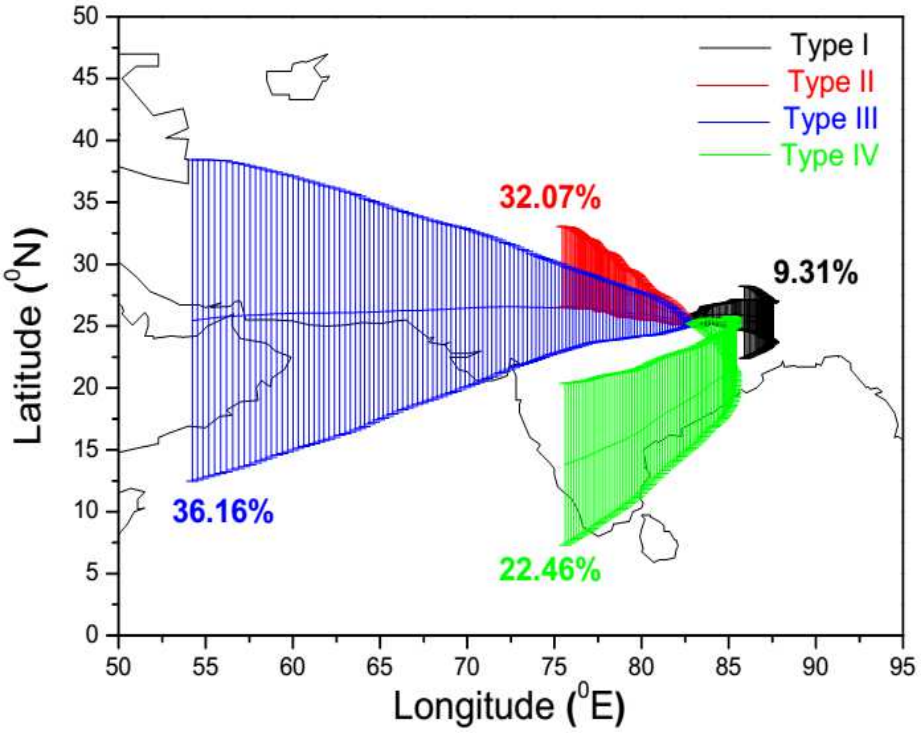

Fig 3: The mean percentage contribution of different air mass types over Varanasi during 2011 (obtained from 5-day air mass back-trajectory analysis from NOAA Hysplit model). The vertical lines show standard deviation, representing latitudinal air mass spreading.

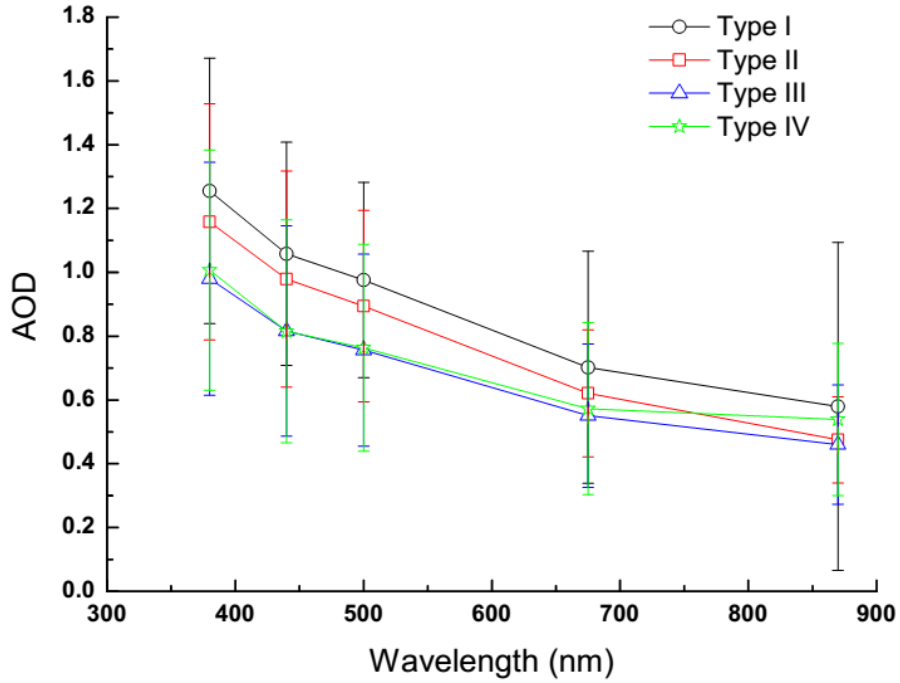

Fig 4: Spectral variation of AOD for different aerosol types during the study period. The vertical lines represent the standard deviation.

the study site. Tiwari *et al.* (2015) reported similar spectral behaviour for different types of aerosol over entire IGB and Srivastava *et al.* (2014) at New Delhi. In another study, Gogoi *et al.* (2009) have done cluster analysis of air mass back trajectories over Dibrugarh in the north-east region, and showed an enhancement in AOD over the station, which was found to be highly associated with the significant transport of mineral dust from the arid regions of west Asia and north-west part of India across the IGB and marine aerosols from nearby marine regions.

The annual mean AOD (at 500 nm) and the corresponding AE (380-870 nm) along with their maximum and minimum values for each aerosol type over Varanasi during the entire study period is given in Table 1. Mean AOD (AE) values for Type I, II, III and IV are 0.98±0.31 (0.93±0.26), 0.89±0.30 (1.06 ± 0.22), 0.76±0.30 (0.92+0.25) and 0.76±0.32 (0.79±0.25) respectively. Kaskaoutis *et al.* (2009) also reported the AOD (AE) value of 0.67±0.13 (1.17±0.12) for heavily urban industrial aerosol including biomass burning, which is smaller to the values observed for Type II aerosol in the present case. Results suggest that although AOD values are nearly same for different Type I, II, III aerosol, their size distribution may be different due to different source emissions. Apart from this, a seasonal pattern in aerosol loading is observed over Varanasi during study period which are given in Table 2 in terms of AOD and AE. Table 2 clearly reflects that in pre-monsoon, Type II and III aerosols have nearly equal values of AOD (AE) with the values of 0.64±0.18 (0.78±0.20) and 0.65±0.25 (0.77±0.19), respectively which indicate the probable mixing state of atmospheric aerosol (Dey *et al.*, 2008; Misra *et al.*, 2014). Srivastava *et al.* (2012) also reported nearly similar AOD (AE) values for polluted dust and polluted continental aerosols 0.63±0.21 (0.45±0.12) and 0.72±0.22 (0.78±0.12), respectively for Gandhi College. Recently, Tiwari *et al.* (2015) found nearly similar AOD (0.64) value but relatively lower AE value (0.44) for polluted dust aerosol over Kanpur which may due to dominance fine mode aerosol particles. Similarly, in post- monsoon season Type I and II aerosols have nearly same AOD (AE) with the values of 1.07±0.36 (1.16±0.11) and 1.02±0.28 (1.2±0.09), respectively which indicate the presence of fine mode aerosols over the station mainly from the biomass burning sources during the period which are well mixed with local anthropogenic aerosols. An interesting feature is observed that during pre-monsoon season, AE value lies below 0.8 (i.e. AE < 0.8) for all types of aerosol indicating the dominance of coarse particles, however in post-monsoon season, AE value have greater value (i.e. AE > 1) for all aerosol type suggesting the dominance of fine particles, which are also confirmed by curvature study of aerosols, discussed in next section.

In support of present assumption, we tried relating aerosol load (i.e. AOD) and particle size (i.e. AE) as suggested elsewhere (Eck *et al.*, 1999; Pace *et al.*, 2006; Kaskaoutis *et al.*, 2007b, 2009, 2011; Kalapureddy *et al.*, 2009; Pathak *et al.*, 2012; Mishra *et al.*, 2014; Tiwari *et al.*, 2015). We found that there is a wide range of AOD and AE values observed for all aerosol types. For Type III aerosols, generally AOD >0.4 along with AE in the range of 0.6-1.2 is found. This suggests existence of polluted continental aerosols which resulted in the enhancement of fine mode aerosol particles. Similar observation is also noticed by Tiwari *et al.* (2015) and Singh *et al.* (2004) over another location, Kanpur, in IGB and by and Srivastava *et al.* (2014) for Delhi. They found similar range of values for polluted continental aerosols over Delhi, with an average value of AOD = 0.62 ± 0.16 and AE = 0.77 ± 0.14. Recently, Tiwari *et al.* (2015) also reported a very close range of AOD and AE (440-870 nm) for polluted continental type aerosol over entire IGB. Type II aerosols, however, show higher AE value (>0.8) with a wide range of AOD (from 0.4 to 1.4) suggesting a mixing of biomass aerosol with anthropogenic aerosol (mainly from fossil fuel). Recently, Tiwari *et al.* (2015) also found nearly similar range for AOD and AE for organic carbon enriched aerosol over Kanpur.

5.2 Curvature Dependency of AOD and AE for Different Aerosol Types

Several studies suggest that difference between second order polynomial cofficient have nearly equal value of angstorm exponent for a given spectral band (Schuster *et al.*, 2006; Kaskaoutis *et al.*, 2009). Therefore, for minimum errors second order polynomial filtting is performed in AOD data set for entire spectral band and their cofficients are calculated. Fig 5 represents the correlation plot between A_2 - A_1 and $AE_{380\text{-}870}$ for different aerosol types over Varanasi during study period. A significatnt correlations ($r \geq 0.98$) were observed for all aerosol types. Thus, applying second order polynomial fitting a good data set is observed which are valid for the data analysis in terms of curvature study.

Fig 6(a) shows scatter plot of curvature coefficient (A_2) against AOD_{500} which provides important information about the dominant aerosol sizes. The negative values of A_2 represent concave type second order polynomial curve which are associated with the dominance of fine mode aerosol particles while positive values represent convex type curve representing dominance of coarse mode aerosol particles. A small positive value of curvature –

Table 1: Annual mean aerosol characteristics for inferred aerosol types at Varanasi during 2011

Aerosol Type	$AOD_{500\ nm}$ (Max/Min)	$AE_{340\text{-}870\ nm}$ (Max/Min)	A_2 (Max/Min)
I	0.98 ± 0.31 (1.71/0.31)	0.93 ± 0.26 (1.31/0.26)	+ 0.22 ± 0.64 (1.62/-0.534)
II	0.89 ± 0.30 (1.67/0.30)	1.06 ± 0.22 (1.37/0.23)	- 0.18 ± 0.48 (1.516/-0.637)
III	0.76 ± 0.30 (1.77/0.22)	0.92 ± 0.25 (1.32/0.25)	+ 0.27 ± 0.48 (1.64/-0.56)
IV	0.76 ± 0.33 (1.71/0.25)	0.79 ± 0.25 (1.42/0.17)	0. 82 ± 0.62 (2.63/-0.38)

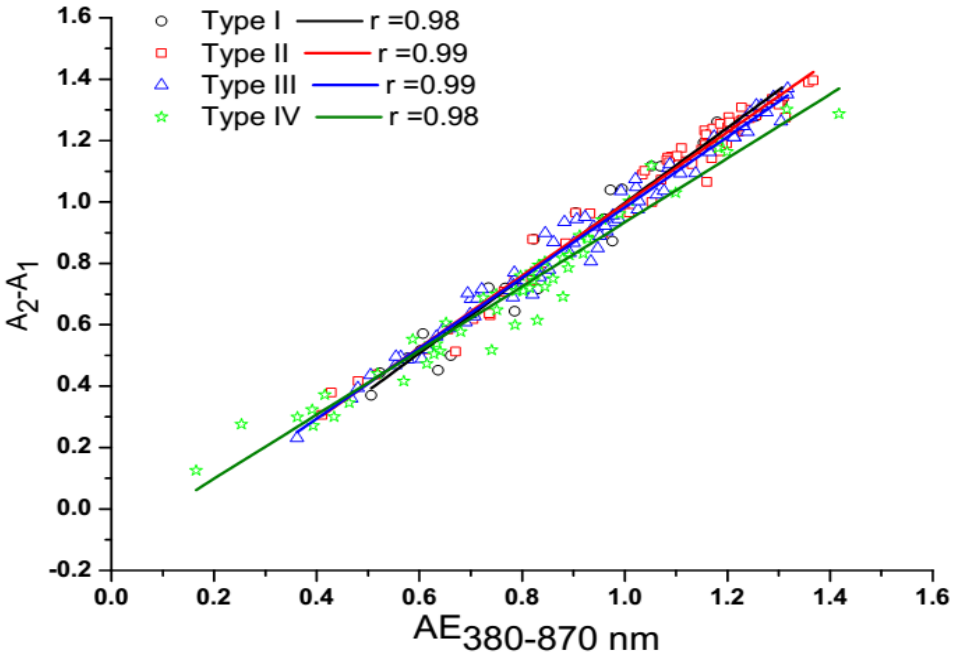

Fig 5: Scatter plot of $A_2 – A_1$ Vs AE (380-870 nm).

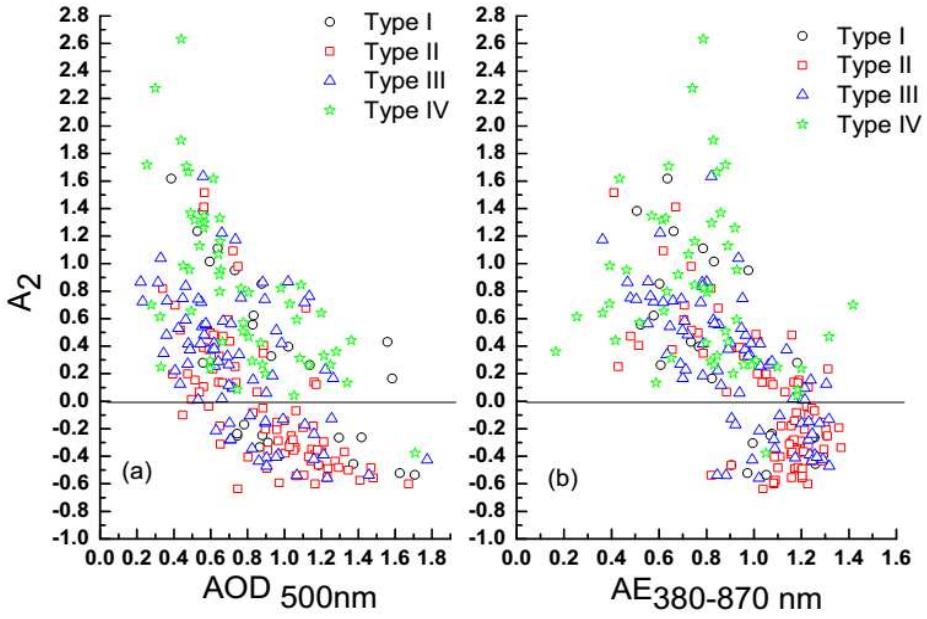

Fig 6: Scatter plot between (a) AOD_{500} and A2 (b) $AE_{380\text{-}870}$ and A_2.

(for AOD_{500} > 0.5) represents the initial fine mode aerosol particles which may be modified from coagulation and gas to particles conversation process (Eck *et al.,* 1999; Schuster *et al.,* 2006; Kaskaoutis *et al.,* 2007). On the other hand, nearly zero values of A_2 represent the mono-modal Jung size distribution or a bimodal lognormal aerosol size distribution without curvature (Eck *et al.,* 1999; Kaskaoutis *et al.,* 2007). Type IV has positive curvature, which indicates bimodal aerosol size distribution with dominance of coarse mode aerosol particles. Similar results are observed over Hyderabad and Arabian Sea by Kaskaoutis *et al.* (2009, 2010). Apart from this, rest three aerosol types have both types of curvature, i.e. positive as well as negative with a large spreading range. Figure reflects that Type II aerosols have majority in negative curvature which indicates dominance of fine mode aerosol particles (mainly from the Northern India, as shown in Fig 3). Recently, Kannemadugu *et al.* (2014) reported negative curvature for urban-industrial/biomass burning aerosol over Nagpur in central India. Kaskaoutis *et al.* (2009) also reported a negative curvature in majority over Hyderabad for urban/industrial aerosol under high aerosol loading during each season except post-monsoon where they observed positive curvature with equal contribution. (Fig 6a) also reflects that Type III aerosols have mostly positive curvature associated with AOD and AE value less than 0.8 and 1.0 respectively (i.e. AOD < 0.8 and AE < 1.0) indicating the dominance of coarse mode aerosol particle (mainly dust aerosol) from the Thar Desert and Middle East regions (Fig 3) due to long range transport. Type III aerosol also have negative curvature associated with the AOD ranging from 0.6-0.8 which refers bimodal lognormal size distribution (Schuster *et al.,* 2006). A similar type of curvature is also observed by Kannemadugu *et al.* (2014) for desert dust aerosols over Nagpur. Observed results in present study are similar to several previous studies performed at different location throughout the world (Eck *et al.,* 1999; Eck *et al.,* 2001; Schuster *et al.,* 2006; Badarinath *et al.,* 2009; Kaskaoutis *et al.,* 2007, 2009).

For further clarification in discrimination of aerosol types, a scatter plot between $AE_{380\text{-}870}$ and curvature is shown in Fig 6(b). In general a specific value of AE (0.5-0.9) was observed for a large spreading in curvature, which indicate a different size distribution with nearly similar AE value to produce a large difference in curvature (Schuster *et al.,* 2006). Result suggests that only curvature may not be able to describe aerosol particle size. The data lying on or near zero curvature line associated with Jung power law distribution and have a range of AE from 0.88 to 1.2. Seasonal variation in aerosol curvature is given in Table 2. During pre-monsoon and monsoon seasons, a postive curvature is observed for all aerosol types, suggesting the enhancement in coarse mode aerosol particles in pre-monsoon and monsoon. However, a negative curvature is observed in post-monsoon and winter season for all aerosol type indicating dominance of fine mode aerosol particles.

5.3 Seasonal Heterogenity in Aerosol Types Contribution

From the Fig 3, we observed that different types of air masses have different contributions over Varanasi. For more precise analysis of their seasonal pattern and altitudnal variation, we calculated the seasonal percenatage contribution of each aerosol type along with their altitudnal variation (Fig 7). Fig 7 clearly reflects that in pre-monsoon season, there exist a mixed-type aerosol loading over Varanasi with higher contribution of Type III aerosol (~40 %), followed by Type II (~26 %), Type IV (~23 %) and Type I (~11%). The dominance of Type III aerosol suggests the long range transportation of air masses to Varanasi. The second highest comntribution (Type II) indicate towards a significant contribution from Northern India mainly known for crop residue burning during pre-monsoon season (Sharma *et al.,* 2014; Sinha *et al.,* 2014). Recently, Srivasrava *et al.* (2012b) and Tiwari *et al.* (2013) have reported significant influence of biomass burning aerosol over entire IGB region during pre-monsoon period. On the other hand, during monsoon season, Type IV aerosols have maximum contribution (58%), which are mainly following the onset pattern of indian summer monsoon from Indian ocean till IGB. Highest contribution from Type-IV aerosols strongly suggest major contribution from oceanic region, mixed with aerosols from central Indian region. Further, Type III aerosols show second highest contribution (33%) during the monsoon, because on some days air masses over the station are reaching from Arabian sea and passing through the Thar Desert region. Type-III is also following the summer monsoon advancement over Indian subcontinent, entering from western azimuth, passing through Arabian Sea. During post-monsoon season, Type II aerosols dominates with 61% contribution, followed by Type I (25%), Type III aerosols (13%) and Type IV aerosols (1 %). The contribution of aerosols during this season are mainly due to the biomass/agrultural crop-residue burning over northwestern IGB (Tiwari and Singh, 2013; Singh *et al.,* 2004; Badarinath *et al.,* 2009; Sharma *et al.,* 2009; Habib *et al.,* 2006; Srivastava *et al.,* 2012; Mishra *et al.,* 2014) along with urban-industrial sources (Srivastava *et al.,* 2014). During winter season, although Type II (46%) and Type III (48%) show -

Table 2: Seasonal mean aerosol characteristics for inferred aerosol types at Varanasi during 2011

Seasons	Aerosols Types	$AOD_{500\ nm}$ (Max/Min)	$AE_{340\text{-}870\ nm}$ (Max/Min)	A_2 (Max/Min)
Pre-monsoon	I	0.87 ± 0.37 (1.58/0.37)	0.70 ± 0.14 (0.98/0.51)	0.82 ± 0.45 (1.62/0.17)
	II	0.64 ± 0.18 (1.12/0.34)	0.78 ± 0.20 (0.44/1.13)	0.60 ± 0.38 (1.52/0.07)
	III	0.65 ± 0.25 (1.26/0.23)	0.77 ± 0.19 (1.24/0.36)	0.54 ± 0.30 (1.22/-0.13)
	IV	0.80 ± 0.24 (1.25/0.45)	0.79 ± 0.22 (1.20/0.39)	0.56 ± 0.37 (1.35/0.04)
Monsoon	I	-	-	-
	II	0.75 ± 0.26 (1.00/0.40)	0.88 ± 0.33 (1.17/0.43)	0.09 ± 0.17 (0.26/ -0.14)
	III	0.81 ± 0.26 (1.22/0.43)	0.85 ± 0.24 (1.31/0.51)	0.51 ±0.48 (1.64/ -0.10)
	IV	0.70 ± 0.34 (1.36/0.25)	0.77 ± 0.28 (1.42/0.17)	1.12 ± 0.63 (2.63/0.14)
Post-monsoon	I	1.07 ± 0.36 (1.71/0.59)	1.16 ± 0.11 (1.31/0.97)	-0.29 ± 0.20 (0.28/-0.53)
	II	1.02 ± 0.28 (1.67/0.49)	1.2 ± 0.09 (1.37/0.91)	-0.22 ± 0.26 (0.48/-0.60)
	III	0.89 ± 0.32 (1.23/0.43)	1.13 ± 0.13 (1.26/0.95)	-0.14 ± 0.35 (0.53/-0.56)
	IV	0.74	1.19	0.085
Winter	I	1.06 ± 0.18 (1.19/0.93)	0.93 ± 0.04 (0.96/0.91)	-0.068 ± 0.56 (0.33/-0.47)
	II	0.97 ± 0.28 (1.47/0.28)	1.15 ± 0.11 (1.36/0.82)	-0.30 ± 0.26 (0.15/-0.64)
	III	0.83 ± 0.34 (1.77/0.22)	1.10 ± 0.18 (1.32/0.72)	-0.11 ± 0.39 (0.87/-0.54)
	IV	1.71	1.05	-0.38

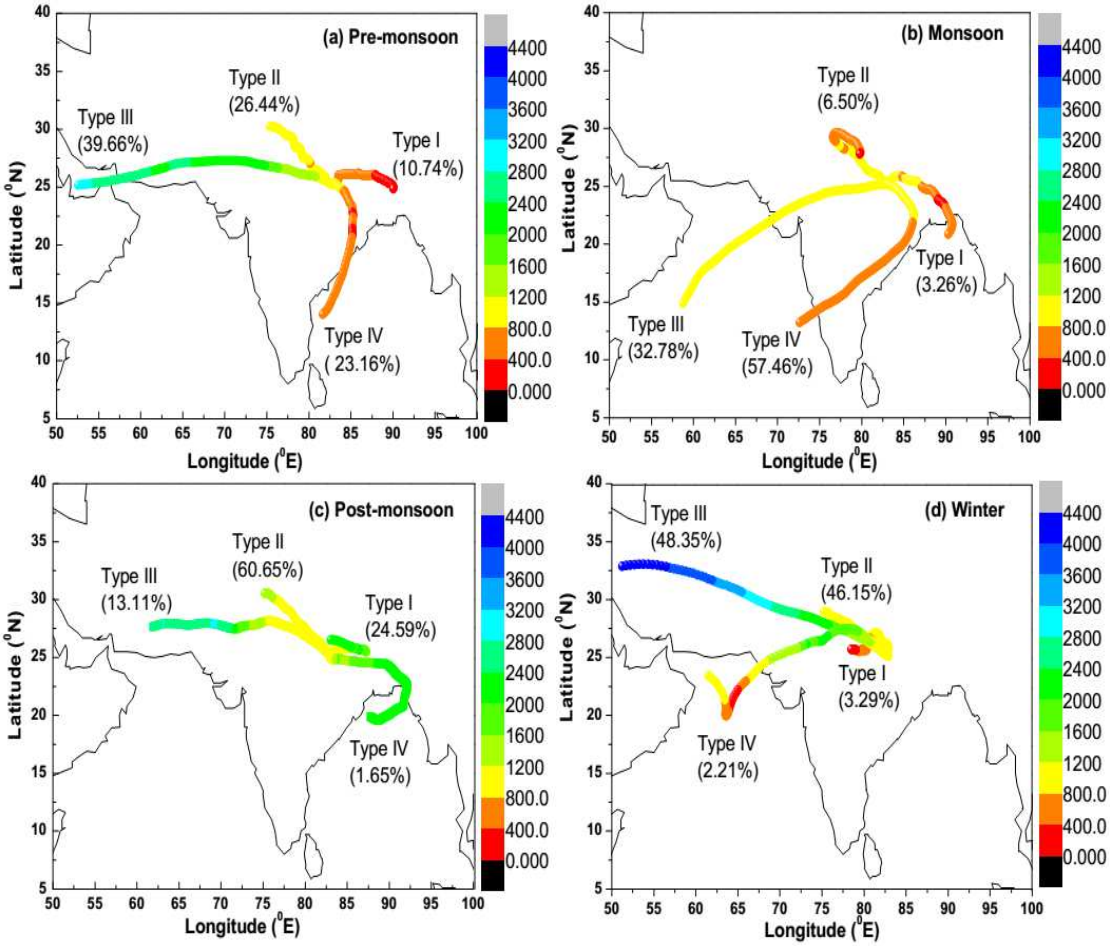

Fig 7: Seasonal percentage contribution of different aerosol types over Varanasi during the study period.

nearly equal contributions, contribution from Type III is found to be transported from southern Europe (Caspean Sea region) and beyond. A closer look, however, suggests that beyond 65^0E longitude in Type III, the air masses are much above the boundary layer altitudes, which is slowly reaching to lower altitudes after at around 65^0E longitudes (Afghanistan/Pakistan). At this altitude, the air masses are expected to accommodate regional/urban pollutants from western IGB, to be noticed with airmass reaching to the Varanasi, contributing fine-mode particles included during the travel from 65^0E till recepter-site. The contribution of Type II, as well as Type III aerosols may be mainly due to local urban-industrial emission from IGB, along with biomass burning, that are responsible for higher contribution of fine mode aerosols.

Atmospheric winds play crucial role in the aerosol loading and their spatial distribution of aerosols. Therefor, to confirm the obtained results, seasonal relationship of AOD and AE with surface winds (speed and direction) is drawn and shown in Fig 8 and Fig 9, respectively. Higher AODs were observed during all the seasons except in post-monsoon when the wind is from western azimuth (west, north west and south west) directions. During pre-monsoon period, for nearly 60% days AODs were lie between 0.6 and 1.2; and for nearly 32% days AODs were between 0.3 and 0.6. On the other hand, for more than 80% days AE was found in between 0.6 and 1.2 and for nearly 16% days, it was between 0.3 and 0.6. Apart from this, during post monsoon/winter season, mostly higher AOD value (>0.9) are associated with the winds coming from northwest, having higher AE values varied between 0.9 and 1.5. From the figure, it is confirmed that during winter season, aerosols are coming mainly from north/northwest direction with relatively higher values of AOD associated with higher values of AE. It indicats admixing of fine mode and coarse mode aerosol particles causing nearly equal contribution of Type II and Type III aerosols over the station in winter season (about 48% and 46%). During the study period, nearly 51% of AOD value lie in a range from 0.9-1.5 associated with nearly 81% of AE value in same range. Recently, Kumar *et al*. (2015) reported that fine mode aerosol particles associated with higher AOD over Varanasi due to long range transportation. However, on the other hand, during post-monsoon season, AOD show a wide range between 0.3 and 1.7, having higher AE, ranging from 0.9-1.36. Results clearly indicate dominance of fine mode aerosol particles as found by air mass back-trajectry analyses and seasonal contribution of inferred aerosol types.

5.4 Climate Impact of Inferred Aerosol

To understand the climate impact of the inferred aerosol types over Varanasi, aerosol radiative forcing was estimated under clear-sky conditions in short-wave region (0.25-4.0 µm) at the surface and top of the atmosphere (TOA) using spectral values of AOD, SSA and Asymmetry parameter (AP) derived from OPAC model as inputs into the Santa Barbara DISORT Atmospheric Radiative Transfer (SBDART) model (Ricchiazzi *et al.,* 1998). Besides these optical parameters, surface albedo and vertical profile of atmospheric parameters (e.g. average temperature, pressure, water vapour and ozone, etc.) for the location are other crucial parameters in SBDART model. Surface albedo, which plays crucial role in forcing estimations, was obtained over the station from Aura OMI version 3 reflectivity data (at 0.50 µm wavelength). However, vertical profile of necessary atmospheric parameters is generally fixed once the model atmosphere is chosen in SBDART. Based on the prevailing meteorological conditions over Varanasi, the tropical model atmospheric profiles have been considered in present study (Singh *et al.,* 2014). The radiative forcing calculations were performed using eight radiation streams to obtain the TOA and surface downward and upward fluxes at every 1-hr interval for a 24-hr period, with and without aerosols. Diurnally averaged radiative forcing at the TOA and surface is thus obtained as difference between net flux (down-up) with and without aerosols. Further, the resultant atmospheric forcing (ΔF) was obtained by the difference between TOA and surface forcing, which represents the amount of solar energy absorbed by aerosols in the atmosphere. Consequently, the atmospheric heating rate is calculated from the first law of thermodynamics and hydrostatic equilibrium (Liou, 2002) as

$$\frac{\partial T}{\partial t} = \frac{g}{C_p} \times \frac{\Delta F}{\Delta P} \times 24(\text{hr/day}) \times 3600(\text{sec/hr}) \quad \cdots (5)$$

where,

$\frac{\partial T}{\partial t}$ is the heating rate in Kelvin per day ($Kday^{-1}$), $\frac{g}{C_p}$ is the lapse rate where g is the acceleration due to gravity and Cp is the specific heat capacity of air at constant pressure (i.e. 1006 $Jkg^{-1}K^{-1}$), ΔF is the estimated atmospheric forcing due to aerosols and ΔP is the atmospheric pressure difference between top and bottom boundaries of the atmosphere in which most of the aerosols occur, which is considered to be 300 hPa in the present study. Though the aerosol radiative forcing has been estimated using model derived aerosol products from OPAC, numerous factors such as scale –

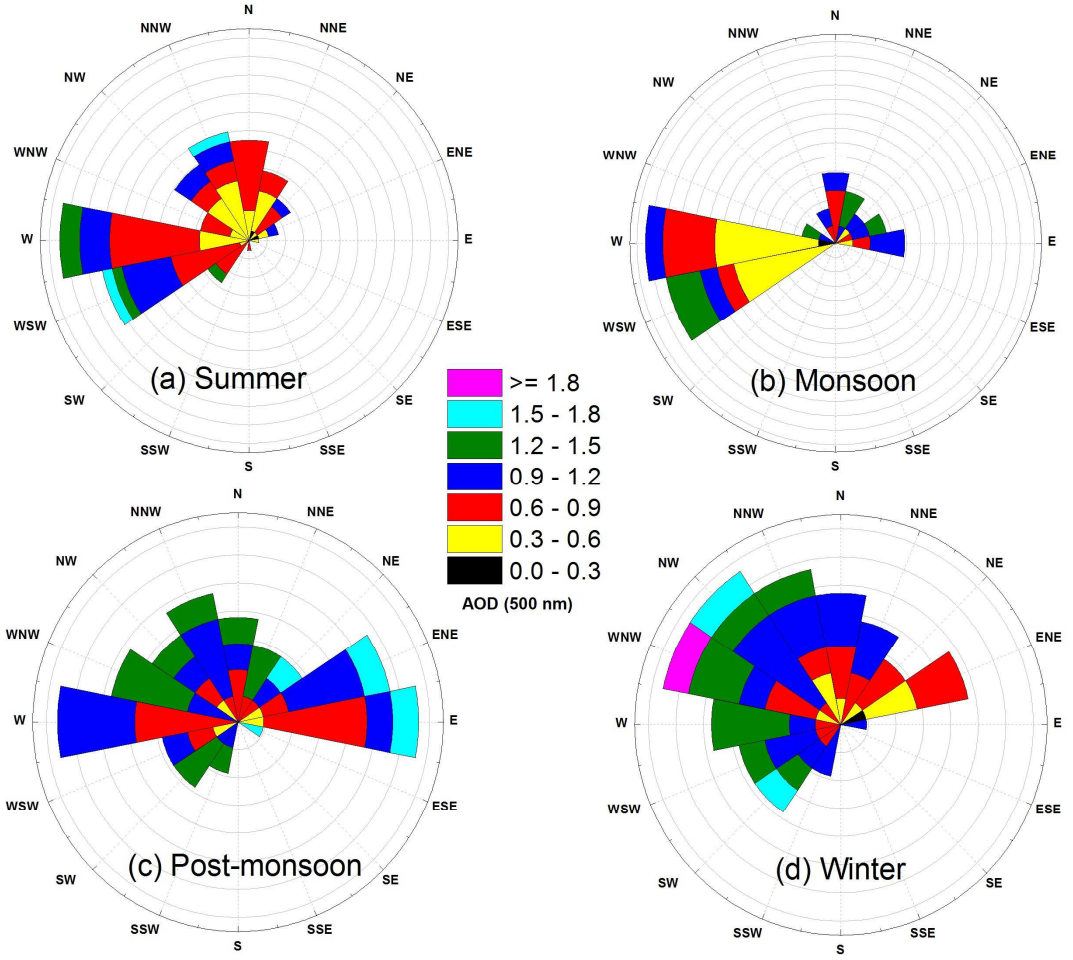

Fig 8: Variation of AOD with wind direction during (a) Summer, (b) Monsoon, (c) Post-monsoon and (d) Winter periods.

height of each species, mixing state of aerosols, surface albedo and sky conditions may also influence the overall uncertainties in radiative forcing estimations (Dey and Tripathi, 2008; Singh *et al.*, 2014) then showed a reduction in scale height from 1.2 to 0.8 km may reduce the AOD by ~10%, enhancing the surface forcing by 2 Wm^{-2} and reducing the TOA forcing by 2.6 Wm^{-2}.

The total uncertainty in the estimated radiative forcing by this method has been reported to be ~15% (Dey and Tripathi, 2008; Srivastava and Ramchandran, 2013) which included the uncertainty in surface albedo. Fig 10 represent the short wave radiative forcing at top of the atmosphere (TOA), Surface and Atmospheric for inferred aerosol type. The radiative forcing at the surface is found to be negative (i.e. show net cooling effect) while in the atmosphere it is positive (i.e. show net heating effect) with relatively larger value resulting to the positive radiative forcing at TOA (i.e. show net heating effect) for all inferred aerosol types. Fig 9 reflect that Type III show high forcing at ATM (102.9 ± 10.7 Wm^{-2}) and TOA (21.7 ± 8.1 Wm^{-2}) with heating rate 2.9 ± 0.3 K day^{-1} followed by Type I (ATM: 100.8 ± 17.8 Wm^{-2} and TOA: 14.8 ± 7.6 Wm^{-2}) associated with maximum surface cooling -86 ± 16.9 Wm^{-2}. Apart from this, minimum (ATM: 93.9 ± 29.4 Wm^{-2} and TOA: 14 ± 7.6 Wm^{-2}) forcing was observed for Type IV aerosol associated with maximum surface forcing (80 ± 30.7 Wm^{-2}). A positive TOA forcing is found for all aerosol type with heating rate from 2.6 ± 0.8 K day^{-1} (for Type IV) to 2.9 ± 0.30 K day^{-1} (for Type III) resulting the net heating effect and suggesting the dominance of fine mode aerosol particles mainly coming from anthropogenic emission and biomass/biofuel burning as discussed above.

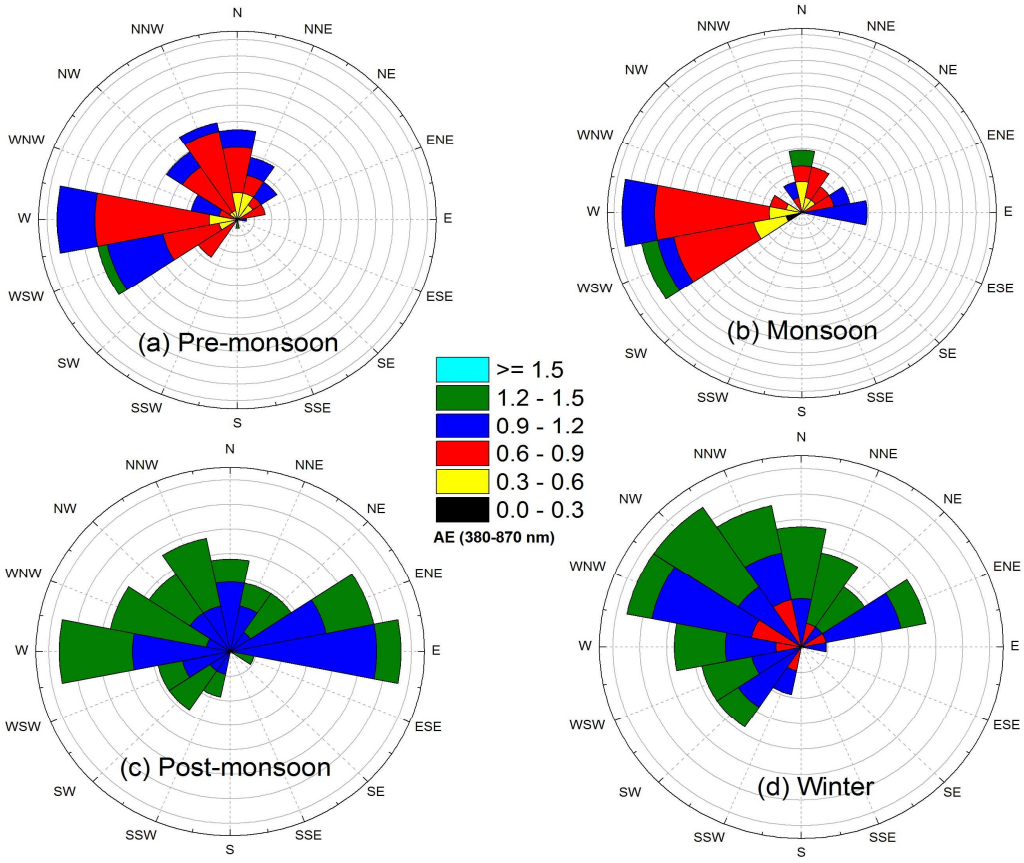

Fig 9: Same as figure 8, except for AE.

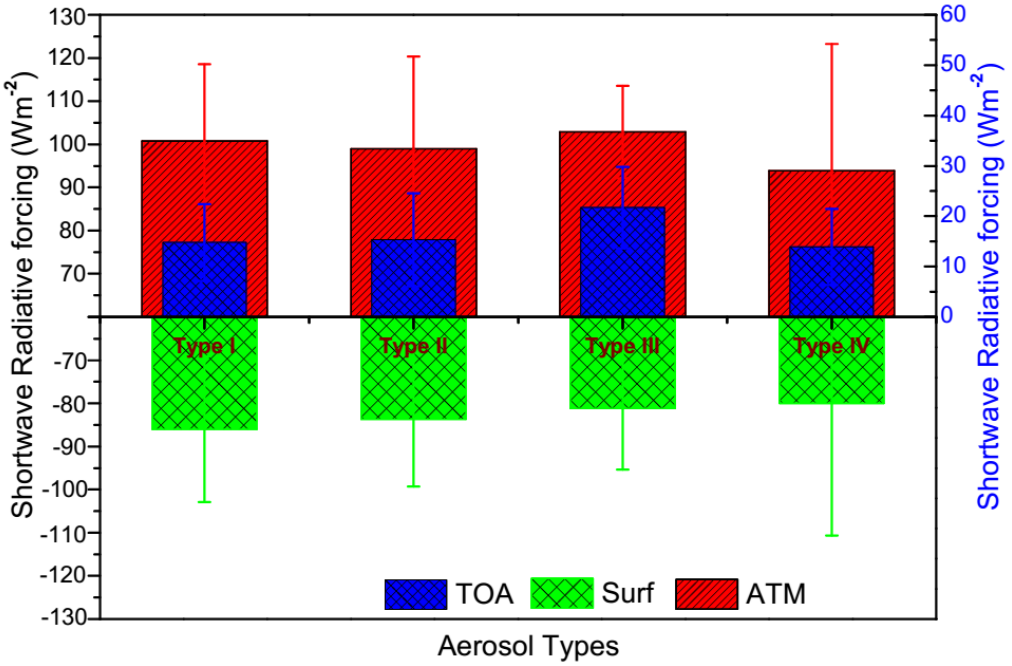

Fig 10: Short-wave radiative forcing at the TOA, surface, and in the atmosphere for the inferred aerosol types.

6. Conclusion

A continuous sunphotometer measurements have been carried out at Varanasi a semi-urban station over the eastern IGB region during 2011 to understand aerosol characteristics. Using air mass back-trajectory analysis, an attempt has been made for the first time to identify different aerosol types and to examine their seasonal heterogeneity over the station. The salient results of the present study are given below:

a) The local emission sources are more important than the long-range transportation over Varanasi which plays a crucial role in favorable meteorological condition.
b) Varanasi experienced a high aerosol loading with annual mean AOD (at 500 nm) varied from 0.73 ± 0.31 to 0.98 ± 0.31 during the study period, with large heterogeneity in different aerosol types due to various emission sources.
c) Four different aerosol types are identified at Varanasi, viz. Type I, Type II, Type III and Type IV based on air mass pathways with their annual contributions of 9.31%, 32.07%, 36.16%, and 22.46%, respectively.
d) The percentage contribution of aerosol types also varies seasonally. During winter and post-monsoon seasons, Type II and Type III aerosols are dominated showing the influence of local sources as well as long range transportation. Type IV aerosols are dominated during monsoon season which are mainly influenced by air masses from the Bay of Bengal and Indian Ocean. However, during pre-monsoon season, station is experienced a mixture of aerosols types.
e) Type I aerosols have maximum annual mean AOD (AE) with values of 0.98 ± 0.31 (0.93 ± 0.26) while minimum is observed for Type III (AOD: 0.75 ± 0.30 AE: 0.92 ± 0.25).
f) The direct aerosol radiative forcing was found to be maximum at ATM and TOA for Type III aerosol with maximum heating rate of 2.89 ± 0.30 K day^{-1}.

Acknowledgement

The author S. Tiwari is thankful to Council of Scientific and Industrial Research (CSIR) for providing senior research fellowship. This work is partially supported by ISRO, Bangalore under ISRO-SSPS and ISRO-ARFI program. We acknowledge HYSPLIT model of NOAA-ARL for back-trajectory analysis.

References

Altaratz O, Koren I, Remer LA and Hirsch E (2014). Review: Cloud invigoration by aerosols - Coupling between microphysics and dynamics, *Atmospheric Research*, 140-141: 38-60.

Ångström A (1964). The parameters of atmospheric turbidity. *Tellus*, 16: 64-75.

Badarinath KVS, Latha KM, Kiran Chand TR, Gupta PK, Ghosh AB, Jain SL, Gera BS, Singh R, Sarkar AK, Singh N, Parmar RS, Koul S, Kohli R, Nath S, Ojha VK and Singh G (2004). Characterization of aerosols from biomass burning - A case study from Mijoram (Northeast), India. *Chemosphere*, 54(2): 167-175.

Badarinath KVS, Kharol SK and Sharma AR (2009). Long-range transport of aerosols from agriculture crop residue burning in indo-gangetic plains-a study using LIDAR, ground measurements and satellite data. *Journal of Atmospheric and Solar-Terrestrial Physics*, 71: 112-120.

Beegum SN, Moorthy KK, Babu SS, Satheesh SK, Vinoj V and Badarinath KVS *et al.* (2009). Spatial Distribution of aerosol Black Carbon over India during Pre-monsoon Season. *Atmospheric Environment*, 43: 1071-1078.

Bibi S, Alam K, Chishtie F and Bibi H (2017). Characterization of absorbing aerosol types using ground and satellites based observations over an urban environment. *Atmospheric Environment*, 150: 126-135.

Das S, Dey S and Dash SK (2015). Impacts of aerosols on dynamics of Indian summer monsoon using a regional climate model. *Climate Dynamics*, 44: 1685-1697.

Dey S, Tripathi SN and Mishra SK (2008). Probable mixing state of aerosols in the Indo-Gangetic Basin, northern India. *Geophysical Research Letters*, 35: L03808.

Dey S and Tripathi SN (2008). Aerosol radiative effects over Kanpur, Indo-Gangetic basin, northern India: Long-term (2001-2005) observations and implications to regional climate. *Journal of Geophysical Research*, 113(D4): 1-20.

Dey S and Di Girolamo L (2010). Climatology of aerosol optical and microphysical properties over the Indian subcontinent from 9 years (2000-2008) of Multiangle Imaging Spectroradiometer (MISR) data. *Journal of Geophysical Research*, 115: D15204.

Draxler RR and Rolph GD (2003). HYSPLIT (*Hybrid Single-Particle Lagrangian Integrated Trajectory*) model. NOAA Air Resources Laboratory, Silver Spring, MD.

Eck TF, Holben BN, Reid JS, Dubovik O, Smirnov A, O'Neill NT, Slutsker I and Kinne S (1999). Wavelength dependence of the optical depth of biomass burning, urban, and desert dust aerosols. *Journal of Geophysical Research*, 104(D24): 31, 333-349.

Eck TF, Holben BN, Dubovik O, Smirnov A, Slutsker I, Lobert JM and Ramanathan V (2001). Column-integrated aerosol optical properties over the Maldives during the northeast monsoon for 1998-2000. *Journal of Geophysical Research*, 106: 28555-28566.

El-Metwally M, SC Alfaro, M Abdel Wahab and B Chatenet (2008). Aerosol characteristics over urban Cairo: Seasonal variations as retrieved from Sunphotometer. *Journal of Geophysical Research*, 113: D14219.

Gautam R, Hsu NC and Lau KM (2010). Pre-monsoon aerosol characterization and radiative effects over the Indo-Gangetic Plains: Implications for regional climate warming. *Journal of Geophysical Research*, 115: D17208.

Gogoi MM, Moorthy KK, Babu SS and Bhuyan PK (2009). Climatology of columnar aerosol properties and the influence of synoptic conditions: First-time results from the north eastern region of India. *Journal of Geophysical Research*, 114: D08202.

Guttikunda SK, Carmichael GR, Calori G, Eck C and Woo JH (2003). The contribution of mega cities to regional sulphur pollution in Asia. *Atmospheric Environment*, 37(1): 11-22.

Habib G, C Venkataraman, I Chiapello, S Ramachadran, O Bopucher and Reddy MS (2006). Seasonal and interannual variability in absorbing aerosols over India derived from TOMS: Relationship to regional meteorology and emissions. *Atmospheric Environment*, 40: 1909-1921.

Holben BN, Tanre D, Smirnov A and Eck TF *et al.* (2001). Emerging ground-based aerosol climatology: Aerosol optical depth from AERONET. *Journal of Geophysical Research*, 106: 12,067-12,097.

Intergovernmental Panel on Climate Change (IPCC). Climate change (2007). The physical science basis: Contribution of working group i to the fourth assessment report of the intergovernmental panel on climate change; 2007 Chapter 2. pp. 129-234.

IPCC: Fifth assessment report: Climate change (2013). Cambridge University Press, New York, NY, USA, 2013.

Jacovides CP, Kassomenos P and Kaltsunideset NA (1996). Estimate of effective aerosol optical depths from spectral solar radiation measurements. *Theoretical and Applied Climatology*, 53: 211-220.

Kalapureddy MCR, Kaskaoutis DG, Ernest Raj P, Devara PCS, Kambezidis HD, Kosmopoulos PG and Nastos PT (2009). Identification of aerosol type over the Arabian Sea in the pre-monsoon season during the Integrated Campaign for Aerosols, Gases and Radiation Budget (ICARB). *Journal of Geophysical Research*, 114: D17203.

Kannemadugu HBS, Joshi AK and Moharil SV (2014). Aerosol optical properties and types over Nagpur, Central India. *Sustainable Environment Research*, 24(1): 29-40.

Kant S, Panda J, Gautam R, Wang PK and Singh SP (2017). Significance of aerosols influencing weather and climate over Indian region. *International Journal of Earth and Atmospheric Science*, 04(01): 1-10.

Kaskaoutis DG and Kambezidis HD (2006). Investigation on the wavelength dependence of the aerosol optical depth in the Athens area. *Quarterly Journal of the Royal Meteorological Society*, 132: 2217-2234.

Kaskaoutis DG, Kambezidis HD, Hatzianastassiou N, Kosmopoulos P and Badarinath KVS (2007a). Aerosol climatology: on the discrimination of the aerosol types over four AERONET sites. *Atmospheric Chemistry and Physics Discuss*, 7: 6357-6411.

Kaskaoutis DG, Kambezidis HD, Hatzianastassiou N, Kosmopoulos PG and Badarinath KVS (2007b). Aerosol climatology: dependence of the Ångström exponent on wavelength over four AERONET sites. *Atmospheric Chemistry and Physics Discuss*, 7: 7347-7397.

Kaskaoutis DG, Badarinath KVS, Kharol SK, Sharma AR and Kambezidis HD (2009). Variations in the aerosol optical properties and types over the tropical urban site of Hyderabad, India. *Journal of Geophysical Research*, 114: D22204.

Kaskaoutis DG, Kharol SK, Sinha PR, Singh RP, Kambezidis HD, Sharma AR and Badarinath KVS (2011). Extremely large anthropogenic-aerosol contribution to total aerosol load over the Bay of Bengal during winter season. *Atmospheric Chemistry and Physics*, 11: 7097-7117.

Kaskaoutis DG, S Kumar, D Sharma, RP Singh, SK Kharol, M Sharma, AK Singh, S Singh, A Singh and D Singh (2014). Effects of crop residue burning on aerosol properties, plume characteristics, and long-range transport over northern India, *Journal of Geophysical Research of Atmosphere*, 119: 5424-5444.

Kaufman YJ, Tanre D and Boucher O (2002). A satellite view of aerosols in the climate system. *Nature*, 419: 415-423.

Kharol SK, Badarinath KVS, Sharma AR, Mahalakshmi DV, Singh D and Prasad VK (2012). Black carbon aerosol variations over Patiala city, Punjab, India-A study during agriculture crop residue burning period using ground measurements and satellite data. *Journal of Atmosphere Science*, 33: 2242-2251.

King MD and Byrne DM (1976). A method for inferring total ozone content from the spectral variation of total optical depth obtained with a solar radiometer. *Journal of Atmosphere Science*, 33: 2242-2251.

Koch D and Del Genio AD (2010). Black carbon semi-direct effects on cloud cover: review and synthesis. *Atmospheric Chemistry and Physics*, 10: 7685-7696.

Kumar M, Tiwari S, Murari V, Singh AK and Banerjee T (2015). Wintertime characteristics of aerosols at middle Indo-Gangetic Plain: Impacts of regional meteorology and long range transport. *Atmospheric Environment*, 104: 162-175.

Lau KM, Kim MK and Kim KM (2006). Asian summer monsoon anomalies induced by aerosol direct forcing: The role of the Tibetan Plateau. *Climate Dynamics*, 26(7-8): 855-864.

Lawrence MG and Lelieveld J (2010). Atmospheric pollutant outflow from southern Asia: a review. *Atmospheric Chemistry and Physics*, 10(22): 11017-11096.

Mishra AK and Shibata T (2012). Climatological aspects of seasonal variation of aerosol vertical distribution over central Indo-Gangetic belt (IGB) inferred by the space-borne lidar CALIOP. *Atmospheric Environment*, 46: 365-375.

Mishra AK, Shibata T and Srivastava AK (2014). Synergistic approach for the aerosol monitoring and identification of types over Indo-Gangetic Basin in pre-monsoon

Season. *Aerosol and Air Quality Research*, 14(3): 776-782.

Misra A, Gaur A, Bhattu D, Ghosh S, Dwivedi AK, Dalai R, Paul D, Gupta T, Tare V, Mishra SK and Singh Tripathi SN (2014). An overview of the physico-chemical characteristics of dust at Kanpur in the central Indo-Gangetic basin. *Atmospheric Environment*, 97: 386-396.

Monkkonen P, Uma R, Srinivasan D, Koponen IK, Lehtinen KEJ, Hameri K, Suresh R, Sharma VP, Kulmala M (2004). Relationship and variations of aerosol number and PM_{10} mass concentrations in a highly polluted urban environment New Delhi, India. *Atmospheric Environment*, 38: 425-433.

Moorthy KK, Nair VS, Babu SS and Satheesh SK (2009). Spatial and vertical heterogeneities in aerosol properties over oceanic regions around India: implications for radiative forcing. *Quarterly Journal of the Royal Meteorological Society*, 135: 2131-2145.

Moorthy KK, Beegum SN, Babu SS, Smirnov A, Rachel S, John Kumar KR, Narasimhulu K, Dutt C and Nair VS (2010). Optical and physical characteristics of Bay of Bengal aerosols during W-ICARB: spatial and vertical heterogeneities in the MABL and in the vertical column. *Journal of Geophysical Research*, 115: D24213.

Morgan MG, Adams PJ and Keith DW (2006). Elicitation of expert judgments of aerosol forcing. *Climate Change*, 75: 195-214.

Morys M, Mims FM III, Hagerup S, Anderson SE, Baker A, Kia J and Walkup T (2001). Design, calibration, and performance of MICROTOPS II handheld ozone monitor and sun photometer. *Journal of Geophysical Research*, 106: 14573-14582.

Pace G, di Sarra A, Meloni D, Piacentino S and Chamard P (2006). Aerosol optical properties at Lampeduca (*Central Mediterranean*) Influence of transport and identification of different aerosol types. *Atmospheric Chemistry and Physics*, 6: 697-713.

Pathak B, Bhuyan PK, Gogoi M and Bhuyan K (2012). Seasonal Heterogeneity in Aerosol types over Dibrugarh North-Eastern India. *Atmospheric Environment*, 47: 307-315.

Pinker RT, G Pandithurai, BN Holben, O Dubovik and TO Aro (2001). A dust outbreak episode in sub-Sahel, West Africa, *Journal of Geophysical Research*, 106(D10): 22, 923-22, 930.

Porch W, Chyleka P, Dubeya M and Massie S (2007). Trends in aerosol optical depth for cities in India. *Atmospheric Environment*, 41: 7524-7532.

Prasad AK, Singh RP and Kafatos K (2006). Influence of coal based thermal power plants on aerosol optical properties in the Indo-Gangetic basin. *Journal of Geophysical Research*, 33(5): 1-4.

Prasad AK, Singh S, Chauhan SS, Srivastava MK, Singh RP and Singh R (2007). Aerosol radiative forcing over the Indo-Gangatic plains during major dust storms. *Atmospheric Environment*, 41: 6289-6301.

Ramanathan V and Ramana MV (2005). Persistent, widespread, and strongly absorbing haze over the Himalayan foothills and the Indo-Ganges plains. *Pure Applied Geophysics*, 162: 1609-1626.

Ramchandran S, Kedia S and Srivastava R (2012). Aerosol optical depth trends over different regions of India. *Atmospheric Environment*, 49: 338-347.

Sarangi C, Tripathi SN, Kanawade VP, Koren I and Pai DS (2017). Investigation of the aerosol-cloud-rainfall association over the Indian summer monsoon region. *Atmospheric Chemistry and Physics*, 17: 5185-5204.

Sarkar S, R Chokngamwong, G Cervone, RP Singh and Kafatos M (2005). Variability of aerosol optical depth and aerosol forcing over India, *Advances in Space Research*, 37(12): 2153-2159.

Satheesh SK, Moorthy KK, Kaufman YJ and Takemura T (2006). Aerosol optical depth, physical properties and radiative forcing over the Arabian Sea. *Meteorology Atmospheric Physics*, 91: 45-62.

Satheesh SK, Suresh Babu S, Padmakumari B, Pandithurai G and Soni VK (2017). Variability of atmospheric aerosols over India. In: Rajeevan M and Nayak S (eds) Observed climate variability and change over the Indian region. *Springer Geology. Springer, Singapore*.

Schmid B and Wehrli C (1995). Comparison of Sunphotometer calibration by use of the Langley technique and the standard lamp. *Applied Optics*, 34(21): 4500-4512.

Schuster GL, Dubovik O and Holben BN (2006). Ångström exponent and bimodal aerosol size distribution. *Journal of Geophysical Research*, 111: D07207.

Seinfeld *et al.* (2016). Improving our fundamental understanding of the role of aerosol-cloud interactions in the climate system. *Proceedings of the National Academy of Sciences*, 113(21): 5781-5790.

Sharma AR, Kharol SK and Badarinath KVS (2009). Satellite observations of unusual dust event over north-east India and its relation with meteorological conditions. *Journal of Atmospheric and Solar-Terrestrial Physics*, 71: 2032-2039.

Sharma M, Kaskaoutis DG, Singh RP and Singh S (2014). Seasonal variability of atmospheric aerosol parameters over greater noida using ground sunphotometer observations. *Aerosol and Air Quality Research*, 14: 608-622.

Sharma D, Srivastava AK, Ram K, Singh A and Singh D (2017). Temporal variability in aerosol characteristics and its radiative properties over Patiala, northwestern part of India: Impact of agricultural biomass burning emissions. *Environmental Pollution*, 231: 1030-1041.

Singh RP, Dey S, Tripathi SN, Tare V and Holben B (2004). Variability of aerosol parameters over Kanpur, northern India. *Journal of Geophysical Research*, 109: D23206.

Singh BP, Srivastava AK, Tiwari S, Singh S, Singh RK, Bisht DS, Lal DM, Singh AK, Mall RK and Srivastava MK (2014). Radiative impact of fireworks at a tropical Indian location: A case study. *Advances in Meteorology*, 2014(197072): 1-8.

Sinha V, Kumar V and Sarkar C (2014). Chemical composition of pre-monsoon air in the Indo-Gangetic Plain measured using a new air quality facility and PTR-MS: high surface ozone and strong influence of

biomass burning. *Atmospheric Chemistry and Physics*, 14: 5921-5941.

Soni K, Singh S, Tanwar RS and Nath S (2011). Wavelength dependence of the aerosol ångström exponent and its implications over Delhi, India. *Aerosol Science Technology*, 45: 1488-1498.

Srivastava AK, Tiwari S, Devara PCS, Bisht DS, Srivastava MK, Tripathi SN, Goloub P and Holben BN (2011). Pre-monsoon aerosol characteristics over the Indo-Gangetic Basin: implications to climatic impact. *Annales Geophysicae*, 29: 789-804.

Srivastava AK, Singh S, Tiwari S and Bisht DS (2012a). Contribution of anthropogenic aerosols in direct radiative forcing and atmospheric heating rate over Delhi in the Indo-Gangetic basin. *Environmental Science and Pollution Research*, 19(4): 1144-58.

Srivastava AK, Tripathi SN, Dey S, Kanawade VP and Tiwari S (2012b). Inferring aerosol types over the Indo-Gangetic Basin from ground based sunphotometer measurements. *Atmospheric Research*, 2012(109-110): 64-75.

Srivastava AK, V Yadav, V Pathak, S Singh, S Tiwari, DS Bisht and P Goloub (2014). Variability in radiative properties of major aerosol types: A year-long study over Delhi-an urban station in Indo-Gangetic Basin. *Science of the Total Environment*, 473-474: 659-666.

Tiwari S, Srivastava AK, Bisht DS, Bano T, Singh S, Behura S, Srivastava MK, Chate DM and Padmanabhamurty B (2009). Black carbon and chemical characteristics of PM_{10} and $PM_{2.5}$ at an urban site of North India. *Journal of Atmospheric Chemistry*, 62(3): 193-209.

Tiwari S and Singh AK (2013). Variability of aerosol parameters derived from ground and satellite measurements over varanasi located in indo-gangetic basin. *Aerosol Air Quality Research*, 13: 627-638.

Tiwari S, Srivastava AK and Singh AK (2013). Heterogeneity in pre-monsoon aerosol characteristics over the Indo-Gangetic Basin. *Atmospheric Environment*, 77: 738-747.

Tiwari S, Srivastava AK, Singh AK and Singh S (2015). Identification Q1 of aerosol types over Indo-Gangetic Basin: implications to optical properties and associated radiative forcing. *Environmental Science and Pollution Research*, 22(16): 12246-60.

Tiwari S, Tiwari S, Hopke PK, Attri SD, Soni VK and Singh AK (2016). Variability in optical properties of atmospheric aerosols and their frequency distribution over a mega city "New Delhi", India. *Environmental Science and Pollution Research*, 23: 8781-8793.

Twomey S (1991). Aerosols, clouds, and radiation. *Atmospheric Environment*, 25: 2435-2442.

Wild M (2009). Global dimming and brightening: a review. *Journal of Geophysical Research*, 114: D00D16.

Zhao H, Zhang X, Zhang S, Chen W, Tong DQ and Xiu A (2017). Effects of agri-cultural biomass burning on regional haze in China: a review. *Atmosphere*, 8(88): 2-9.